Lab 5: Extragalactic Astronomy and the Intensity Profiles of Galaxies

Andy Friedman [1,2]

December 7, 2001

ABSTRACT

In this report we discuss Infrared Observations of 8 galaxies with a variety of morphologies (ngc1637, ngc7741, m95, ngc7331, ngc7457, m015, and ngc2775), as well as one edge on spiral with an apparent dust lane (ngc891). We used the familiar techniques of telescope rastering and image calibration, and created aligned mosaics of our images. For optimal image quality, all galaxies were observed in the H band with the exception of ngc891, which was observed in the K, H, and J bands. This allowed us to create a tricolor image of ngc891 and make an extinction map (color-color diagram) of its dust lane. From our mosaics, we created contour plots of all the galaxies which display isophotes, or rings of constant intensity, scaled according to signal to noise. We then created Intensity vs. Radius plots for all galaxies except ngc891, and qualitatively observed the theoretical deVaucoleur's and exponential fits to the bulge and disk components, respectively. These plots involved "deprojecting" the galaxy to correct for the fact that it may be inclined along our line of sight. We also had to use the galaxy's distance and the angle it subtends to convert to a physical distance in kpc for the galactic radius. We find a range of peak H band intensities toward the galactic centers of 11.7 - 16.4 μ_H $(mag/\Box'')$. Extrapolating the disk components of the spirals galaxies back to the galactic center did not conclusively tell us whether Freeman's Law holds in the H-band. From Freeman's Law in the B-band, $I_B(0) \approx 21.7\mu_B$, the assumption of K-III Giant colors for galaxies leads to a Freeman's Law in the H-Band of $I_H(0) \approx 16.8\mu_H$. We find only 3 out of 5 spirals with an extrapolated $I_H(0) \approx 16.8\mu_H$ to within the errors. Finally, we generated an extinction map of ngc891, finding an average visual extinction in the dust lane of $A_V \approx 7 \pm 1\ mags$.

[1] e-mail: friedman@ugastro.berkeley.edu

[2] Lab Group: John, Lauren, Chris, Kirsten, Lee, Jim, Christina, Lindsey, Amy, Shane, Eric, Neil, Dana.

1. Introduction: Intensity vs. Flux

In previous labs, we measured light signals from point sources (i.e. stars), and characterized them in terms of flux, which has cgs units of $erg\ s^{-1}\ cm^{-2}$. [3] The star is a point source because it is too far away to resolve. If it was closer to us (like the sun is), we would be able to resolve its disk and we could no longer characterize it as a point source. Thus we need a new quantity in addition to flux to characterize light signals from objects we can resolve, or what astronomers call, "extended objects".

Since galaxies are resolvable even at great distances, they thus fall under the category of extended objects and must be characterized by something other than flux. The quantity astronomer's use is intensity, which measures the flux as it changes over the spatial extent of the star. For point sources, we disregard all spatial information and integrate all the light over the entire aperture. For galaxies, we preserve this spatial information by asking how much flux falls within a given solid angle. From this, we see that the units of intensity are simply flux per solid angle, or in cgs units, $erg\ s^{-1}\ cm^{-2}\ sr^{-1}$, where the solid angle can be measure in steradians sr, or square arcseconds $\square''$, or any other measure of angular area. Thus flux is simply intensity integrated over solid angle, which is exactly what we did for aperture photometry when we integrated, or counted up, all the starlight in the aperture.

The measurement of intensity will depend specifically on how your detector quantizes patches of sky in its field of view. For the infrared camera, the sky is naturally divided up into pixels. The pixel size is analogous to bin size on a histogram. The larger the solid angle of the pixel, the more counts get included; and vice versa for small pixels. So it becomes a choice between smaller pixels with increased resolution and larger pixels with increased collecting area. Each pixel array detector has a characteristic plate scale which tells you the effective angular size of the patch of sky seen by a pixel. If you built your pixel to cover the earth's surface, you would see the entire sky. Fortunately, the pixels in the IRCAM are roughly 40 micron sized squares that are not nearly as ridiculous as making the earth into a pixel. When we work out the geometry of the size of a patch of the sky subtended, as seen from the perspective of a pixel, we find that for the Leuschner IRCAM, a pixel has an effective angular size of $1.35''$. Since the pixel is square in shape, this leads to an effective angular area of $(1.35'') \times (1.35'') \approx 1.82\ \square''$ in a pixel. From this, we can derive the solid angle in steradians subtended by the pixel.

$\square$

Table 1: *The IRCAM pixel. Notice the square shape. Each side has an effective angular size on the sky of* $1.35''/pixel$*, which gives an effective solid angle of 1.825* $\square''/pixel$*. In reality, since the IRCAM uses a 256* $\times$ *256 pixel array that fits on a 1 cm* $\times$ *1 cm chip, a single pixel has a physical size of roughly* $1\ cm/256 \approx 4 \times 10^{-5} m$*, or roughly 40 microns. Thus this pixel is only a scale model.*

[3] We can also speak of specific flux in a given bandpass which has units of $erg\ s^{-1}\ cm^{-2}\ Hz^{-1}$.

1.1. Converting Between Steradians and square arcseconds in an IRCAM pixel

Steradians (sr) and square arcseconds ($\square''$) are both units of solid angle. It is relatively straightforward to derive the conversion factor between them, so I will quickly outline it here. Beginning with the fact that in a circle, there are $360^o = 2\pi\ rad$, we know that $1\ rad = \frac{360^o}{2\pi} = 57.3^o$. To convert to solid angle, we use the definition of a *steradian* or (sr)

$$1\ sr = (1\ rad)^2 = (57.3^o)^2 \approx 3283\ \square^o \tag{1}$$

So we now know the conversion between sr and $\square^o$. To convert to $\square''$, we use.

$$sr = 3283\ \square^o \times \left(\frac{60'}{1^o}\right)^2 \times \left(\frac{60''}{1'}\right)^2 = 4.25 \times 10^{10}\ \square'' \quad \Rightarrow \tag{2}$$

$$1\ sr = 4.25 \times 10^{10}\ \square'' \ \ or \ \ 1\ \square'' = 2.35 \times 10^{-11}\ sr \tag{3}$$

Another interesting thing to calculate from this is the number of square degrees in the entire sky. Knowing that the entire sky takes up an angle of $4\pi\ steradians$, we can write.

$$\left(\frac{4\pi\ sr}{whole\ sky}\right) \times \left(\frac{3283\ \square^o}{1\ sr}\right) \approx \left(\frac{41252\ \square^o}{whole\ sky}\right) \tag{4}$$

Using our conversion factor from equation 3, we also see that

$$\left(\frac{4\pi\ sr}{whole\ sky}\right) \times \left(\frac{4.25 \times 10^{10}\ \square''}{1\ sr}\right) \approx \left(\frac{5.35 \times 10^{11}\ \square''}{whole\ sky}\right) \tag{5}$$

This is useful for the Leuschner Infrared camera because we can now use the IRCAM's plate scale of $\frac{1.35''}{pixel}$ to find the solid angle on the sky seen by each pixel in both $\square''$ and sr. First note that the angular area of a (square) IRCAM pixel is simply given by the square of the plate scale

$$\left(\frac{1.35''}{pixel}\right)^2 \approx \left(\frac{1.82\ \square''}{pixel}\right) \tag{6}$$

Again we can use equation 3 to find the number of sr in an IRCAM pixel

$$\left(\frac{1.82\ \square''}{pixel}\right) \times \left(\frac{2.35 \times 10^{-11}\ sr}{1\ \square''}\right) \approx \left(\frac{4.28 \times 10^{-11}\ sr}{pixel}\right) \tag{7}$$

As we will see, these conversion factors will be useful when we calculate intensity I (or surface brightness) values per pixel for extended sources in both cgs units $[I] = [ergs^{-1}cm^{-2}sr^{-1}]$ or in the galactic astronomers' preferred units of $[I] = [\mu_B] = [magnitudes/\square'']$ (or μ_H for optimal infrared observations of galaxies).

1.2. Magnitudes Per Square Arcsecond: The Galactic Astronomer's Favorite

With a pixel value in flux like units of $[counts/s]$ or $[ergs/s]$[4], it is relatively straightforward to convert to intensity units of say, $[counts/s\ \Box'']$. We simply divide by the solid angle of a pixel, which for the IRCAM, we have seen is $(1.82\ \Box''/pixel)$. However, given a pixel value in magnitudes, it is not as obvious how to convert to an intensity in units of mag/$\Box''$ First let us go back to the definition of magnitudes.

$$m = -2.5\ log\left(\frac{F}{F_o}\right) \tag{8}$$

where F is the flux of your star and F_o is some reference flux (maybe the flux of Vega). Similarly, for intensity measured in magnitude-like units

$$\mu = -2.5\ log\left(\frac{I}{I_o}\right) \tag{9}$$

Where I if the intensity of your object and I_o is some reference intensity. Since $I = F/\Omega_{pixel}$ and $I_o = F_o/1\Box''$, we find the relation

$$\mu = -2.5\ log\left(\frac{(F/\Omega_{pixel})}{(F_o/1\Box'')}\right) \quad \Rightarrow \quad \mu = m - 2.5\ log\left(\frac{\Omega_{pixel}}{1\Box''}\right) \tag{10}$$

given the Leuschner plate scale, $\Omega_{pixel} = 1.82\ \Box''$, we find the simple relation

$$\mu = m - 0.65 \qquad \left[\frac{mag}{\Box''}\right] \tag{11}$$

This tells us that for relatively dim sources, we can extend our intuition about magnitudes over to mag/$\Box''$, because subtracting a small number like 0.65 means they will have similar numerical values. For example, a standard star of 14th magnitude in J (from aperture photometry) corresponds to a pixel value of 13.35 mag/$\Box''$ in J. This will be useful when we eventually talk about Freeman's law and the relationship between $\mu_B - \mu_H$ and $B - H$. To see how to convert from intensity μ in $magnitudes/\Box''$ to intensity in cgs units, see the appendix or Lindsey's Lab5 Report.

2. Observations

Using familiar techniques, we took infrared images with the Leuschner Telescope and Infrared Camera over the course of several nights. We calibrated the images with the techniques of dark subtraction, sky subtraction, and flat fielding, using previous software and techniques nearly identical to previous labs, with the exception of the sky subtraction. In the case of an extended source such as a galaxy, it is not sufficient to use the median of your science image as the estimate of the sky background, because galaxies are not point sources. The median of a galaxy that subtends

[4]integrating over area of the detector removes the cm^{-2} units

a significant portion of your field of view will likely reflect the presence of some galaxy light, not just sky light. Thus we must dither the telescope and take dedicated sky images off the galaxy to estimate our sky brightness. This will be discussed in more detail in the discussion of the determination of the intensity of the sky and in the galaxy photometry section. For further details on the image calibration process, I refer to Jim Brennan' lab report.

We observed a total of 8 galaxies including: ngc1637, ngc7741, m95, ngc7331, ngc7457, m015, and ngc2775 in H band along with ngc891 in all 3 bands (K,H,J). H band is the optimal infrared band in which to observe galaxies for practical reasons. It happens that H band galaxy images have a higher signal to noise as compared to the K and J bands for several reasons. First of all, the sky is quite noisy in K due to the series of narrow K band emission lines of OH^- radicals in the earth's atmosphere. In addition, the galaxies we wish to image are observed to have the colors of a K(III) giant star, which in the infrared are roughly $J - H \approx 0.8$ and $H - K \approx 0.2$. This means that Galaxies tend have a larger difference between J and H than between H and K, and thus emit more of their light in the longest infrared wavelengths. Thus to observe galaxies optimally, we wish to go as far into the infrared as we can (toward the longest wavelengths) without hitting the K part of the infrared where the sky is particularly noisy. Since J is not far enough into the infrared and K is dominated by sky emission, we compromise by observing in the H band. By comparing individual images in each of the filters (ideally with identical effective exposure times), it is easy to see that the H band images have the highest signal to noise, as shown below.

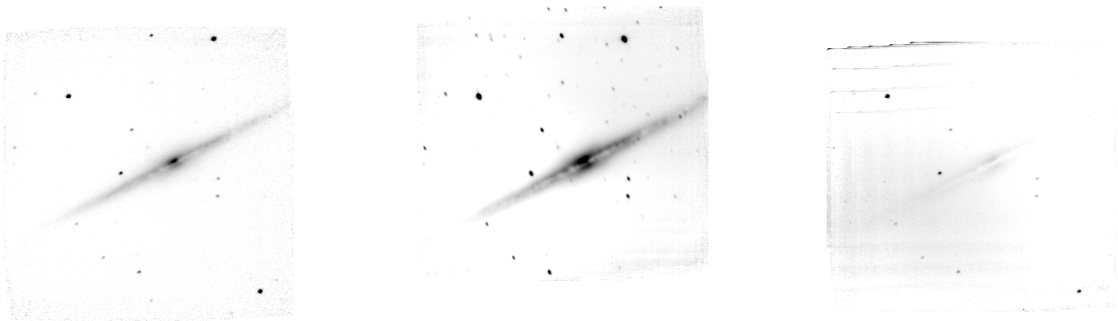

Fig. 1.— From left to right, K, H, and J filter mosaic images of ngc891. The H band images clearly appear to show the highest signal to noise. However, the comparison is not completely fair since we were not able to make mosaics with the same number of images and total effective exposure times. We observed 50 images in K, 50 in H, and 25 in J, with individual exposure times of 30 seconds in J and H, and 10 seconds in K (since K saturates quickly due to the high sky brightness). This gives total effective exposure times toward the center of the raster pattern of 500s in K, 1500s in H, and 750s in J. But suffice it to say, if the total effective exposure time were equal in all bands, the H band image would still show the highest signal to noise by visual inspection.

2.1. Galaxy Images

As shown below, the galaxy's in our sample have a variety of morphological structures.

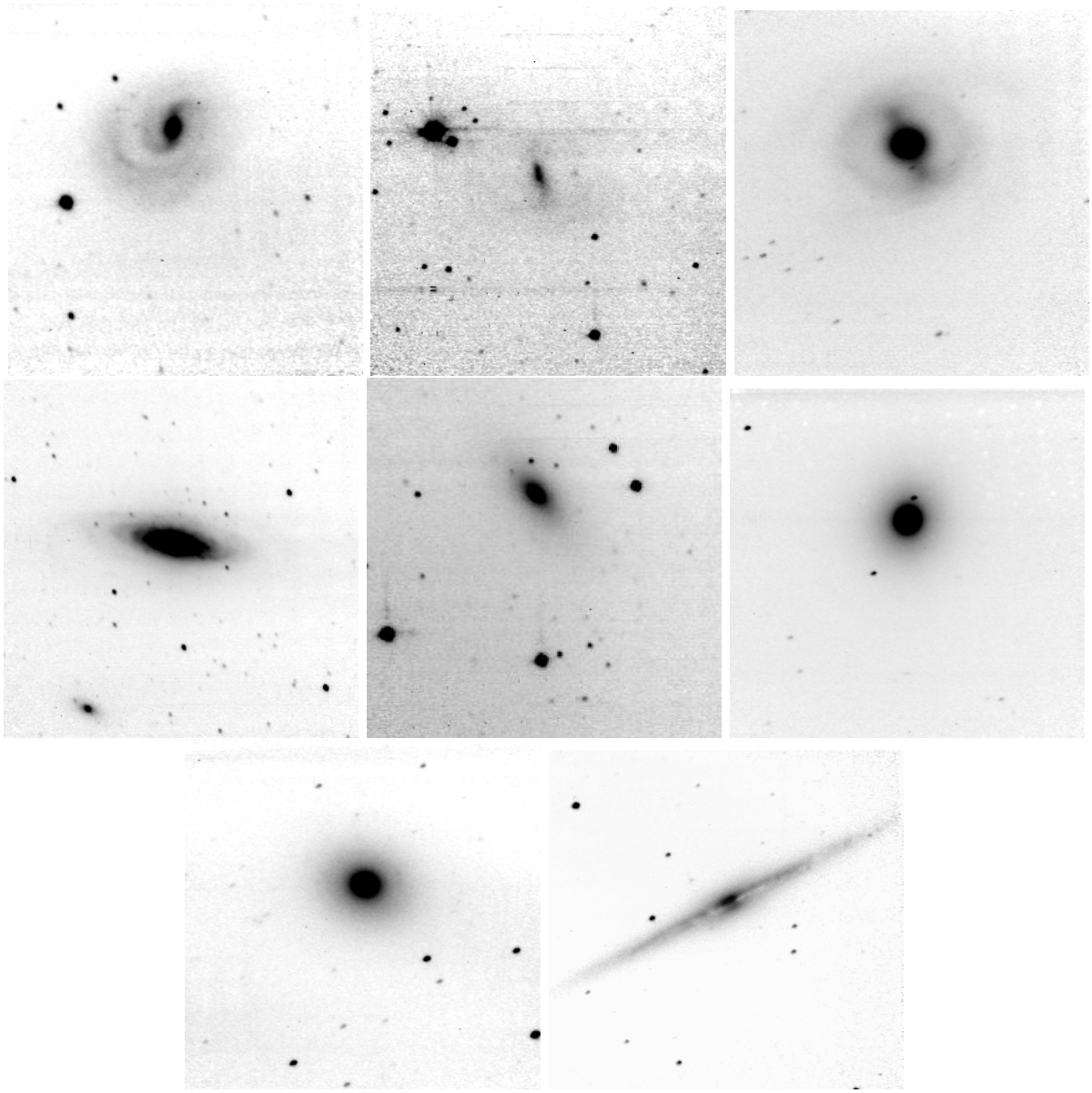

Fig. 2.— From Left to right, top to bottom we have H band mosaics of:
□ (ngc1637: One Armed Sc Spiral), (ngc7741: Sbc Spiral), (m95: Barred Spiral)
□ (ngc7331: Sb Spiral), (ngc7457: S0 Lenticular), (m105: Elliptical)
□ (ngc2775: S0 Lenticular), and (ngc891:Edge on spiral).
Mosaics all constructed using a raster pattern of 49-50 images at 20 seconds per exposure, for a total effective exposure time toward the center of the raster pattern of 1000 s $\approx$ 17 minutes.

3. Sky Brightness

The earth's atmosphere emits a significant amount of light in the infrared, especially in the K band, as mentioned previously. This makes it extremely useful to quantify the brightness of the sky in all three infrared bands to help us to further determine what band to observe in. In previous labs, we used aperture photometry to add up the light coming from our star alone and compared it to the starlight we detect from a standard star of known magnitude using the same size aperture. Conceivably, we could also do this for a blank patch of sky devoid of stars by constructing an aperture, measuring the number of counts inside, and converting to magnitudes using a standard star measured with the same aperture. However, it should be noted that in this situation, we clearly don't need to do sky subtraction in an annulus or moat surrounding our aperture, since the sky is what we are trying to measure in the first place! If we were to subtract the median sky value in our annulus normalized to the number of pixels in our aperture, we would get zero counts for our photometry to within the error of Poisson noise. Sky subtracting the sky would only measure the variance from Poisson noise, it would not give us any photometric information. Thus all we need to do is sum up the sky counts in our aperture.

However, if we perform standard aperture photometry on the sky (with no moat), we notice an inconsistency. The number of counts in your aperture will change as the size of your aperture changes! In fact, if the sky is approximately uniform, the number of counts will increase uniformly as the number of pixels in your aperture increases. Thus if we were to convert that number of counts to a magnitude using a standard star, we would get different values for different sized apertures, as the spatial information of the aperture is effectively collapsed to a single pixel. So how do we resolve this?

The basic problem we are running into is that the sky is not a point source. It is an extended object that, in fact, extends over the entire filed of view of your image, as is unavoidable for ground based observations. Thus as an extended object, its light must be characterized by intensity rather than flux. To do this, we perform moat free aperture photometry on the sky and our standard star, getting a value of counts/s in each pixel, but we make sure to divide by the solid angle subtended by our aperture to put it into intensity units rather than flux units. In effect, we normalize to the size of our aperture. This ensures that the intensity values we find will be independent of aperture size. Another rough way to do this is simply to take the median of your sky image to get a median value of counts/s in each pixel, then convert that value to the galactic astronomer's favorite unit of $mag/\Box''$, using the technique outlined in the previous section.

We used this latter technique for a control field from lab4 and for a patch of sky in the lower left corner of ngc891 in images from all 3 bands. We arrived at a median sky intensity in each band as listed in the table below. Certainly the sky intensity can change from night to night, and as we have seen, even over a timescale of a few minutes. Nevertheless, these values we derived (thanks to Shane and Eric) using images from clear nights several weeks apart, and should thus give us an order of magnitude (no pun intended) idea of the sky brightness in all 3 near infrared bandpasses.

		(control field lab4)	(ngc891 lower left corner)
Band	Central Wavelength (μm)	Median Intensity (μ_H)	Median Intensity (μ_H)
K	2.19	10.5	10.4
H	1.65	12.8	12.8
J	1.22	12.4	12.5

Table 2: *Band, wavelength, and measured median sky intensity using a control field from lab 4, and using a patch of sky in the lower left corner of our ngc891 images. Notice that, as expected, the sky is brightest in K due to the emission of OH^- radicals in the atmosphere, and dimmest in J, with H as the compromise in between. From this alone, it might be argued that we should image galaxies in the J band as opposed to H, since the sky is dimmest in J. This would be a good idea if the galaxy was as bright or brighter in J than in H. Unfortunately we observe galaxies to have the color of K(III) giant stars that have $J - H \approx 0.8$, which qualitatively tells us that $J > H$, and thus the galaxy is dimmer in J than in H. Thus the fact that the galaxy is brighter in H compensates for the fact that the sky is dimmer in J, leaving H as the optimal band for viewing galaxies. Notice also that even though the galaxies are actually brighter in K with a K(III) giant color of $H - K \approx 0.2$, the sky is so much brighter in K as to overwhelm that effect. Thus the galaxy is not bright enough in K as compared to H to make it worth it observe them in K. This also tells us that the galaxies we observed (with peak intensities ranging from 11.7 - 16.4 μ_H as discussed later) would be nearly impossible to detect if we did not perform sky subtraction and make a mosaic with a large effective exposure time. Indeed, this is why we can't see these galaxies with the naked "infrared eye". The sky is simply much brighter in the infrared, where it is always "daytime".*

Fig. 3.— As a completely unabashed space filler, when John was observing from home remotely on the night of the peak of the Leonid Meteor storm, we seem to have caught a meteor streaking across the IRCAM field of view. There's no way to tell whether we caught a short lasting one at the beginning of the exposure or a long lasting one at the end, only that it was there for some portion of our 10 second exposure. But in any case, we think this meteor would have been too faint to see with the naked eye, so, as they'd say in Australia, "Good on you John!"

4. Galaxy Photometry

Integrating the light over the aperture for a standard star effectively tells us how much light would have landed in a single pixel if the atmosphere and the optics were perfectly well behaved and never altered the photon's path. Imperfections in the optics and atmospheric turbulence lead to an effective point spread function which smears out the starlight over several pixels. We correct with this smearing in aperture photometry but summing up all the counts inside the same aperture for both our target and standard star, and converting the counts of our target star to magnitudes. Extended objects such as galaxies, on the other hand would not have their light fall on a single pixel even if the optics were perfect and the atmosphere was gone. Therefore, we expect there to be some spatial distribution of galaxy light on the pixels, and it is not as important to deduce which pixel was supposed to collect the light from which point source (star) in the galaxy. Indeed, since galaxies are so far away, it is practically impossible to resolve a single star, which means we expect light from several million stars (For an average galaxy of 10^{11} stars sub-tending 10% of your field of view of $\approx$ 65000 pixels) to fall on each pixel. Thus for galaxy photometry, we do not need to convolve our galaxy image. We simply look at the mosaic image with pixel values in units of counts/s and use a standard star to convert that value to magnitudes/pixel. Each individual science image has already been sky subtracted, so the mosaic should consist of only galaxy light plus Poisson noise.

We still could do aperture photometry on the galaxy image if we were to convolve the image with a larger kernel that is only a top hat, strictly leaving out the moat. We could no longer use a kernel with a moat since this would artificially subtract off galaxy light. For standard stars, this was OK because the moat (or sky annulus) was located well outside of 3-σ where it could hardly remove any starlight since for a Gaussian star profile, 99% of the starlight falls inside the 3-σ aperture. But it is much simpler to perform galaxy photometry without convolution simply by taking the individual counts/s value in each pixel of the sky subtracted mosaic and converting to magnitudes/pixel using your standard star. When galaxy photometry is completed, we now have the intensity in each pixel, which we can convert to whatever units we want, such as $mag/\Box''$.

5. Contour Plots: Isophotes

Given per pixel intensity values for our galaxy, an interesting way to display galactic structure involves creating contour plots. The contour lines are called isophotes and they mark lines of constant intensity, revealing a structure similar to a topographical map. It would not be meaningful to scale the contour lines arbitrarily, so we decided to scale them according to multiples of the rms noise (or standard deviation) value of the sky background. If the galaxy signal is much greater than the rms noise of the sky, we will be able to detect that galaxy signal. Near the center of the galaxy, (which is near the center of our raster pattern), the galaxy is bright and the signal to noise is high. By contrast, the signal to noise is much smaller toward the edges where the pixels received less effective exposure time and where the galaxy itself is dimmest as the number of stars declines towards the edges and the peripheral starlight fades into the sky background.

Thus one way of characterizing the edge of the galaxy is to look at the isophote corresponding to a signal to noise value of 1, where the intensity of that isophote equals the rms noise of the sky. This is the limit beyond which we can no longer detect stars in the galaxy in the presence of the sky background, and it allows us to reasonably specify where the galaxy effectively ends by visual inspection. Even so, since the number of stars in the galaxy fall off exponentially as we reach the edge, an isophote with intensity equal to 2, 3, or even 4 times the rms value can also be reasonably used to give us a lower limit estimate the edge of the galaxy. On the following pages we display contour plots for m105 next to the galaxy image for comparison, to show two ways to estimate the edge of the galaxy. We then display the contour plots for all 8 galaxies and we specify the rms and the multiples were used to determine the edge and the levels of the contour plot.

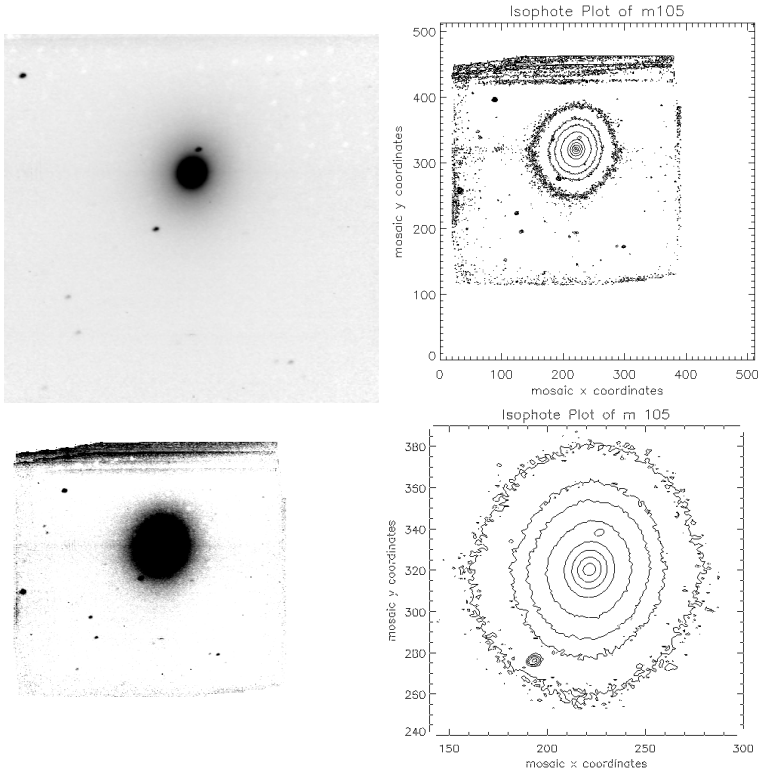

Fig. 4.— The Elliptical galaxy m105 shown in our mosaic image (upper left) along with its contour plot (upper right). Notice that we can see structure much further out from the galactic center in the contour plot. The appearance of the galaxy image edge especially is extremely sensitive to your choice of tv scaling. Thus it is often more useful to use the contour plot to estimate the location of the edge of the galaxy. However, with very narrow tv scaling values such as >0 <1 as in the galaxy image on the (lower left), one can estimate the edge of the galaxy to similar accuracy. We used this method when converting the angular size of the galaxy to a physical size in kpc. The (lower right) corner is a zoomed in contour plot of the galaxy, with array coordinates on the x and y axes.

6. Contour Plots of Our 8 Galaxies

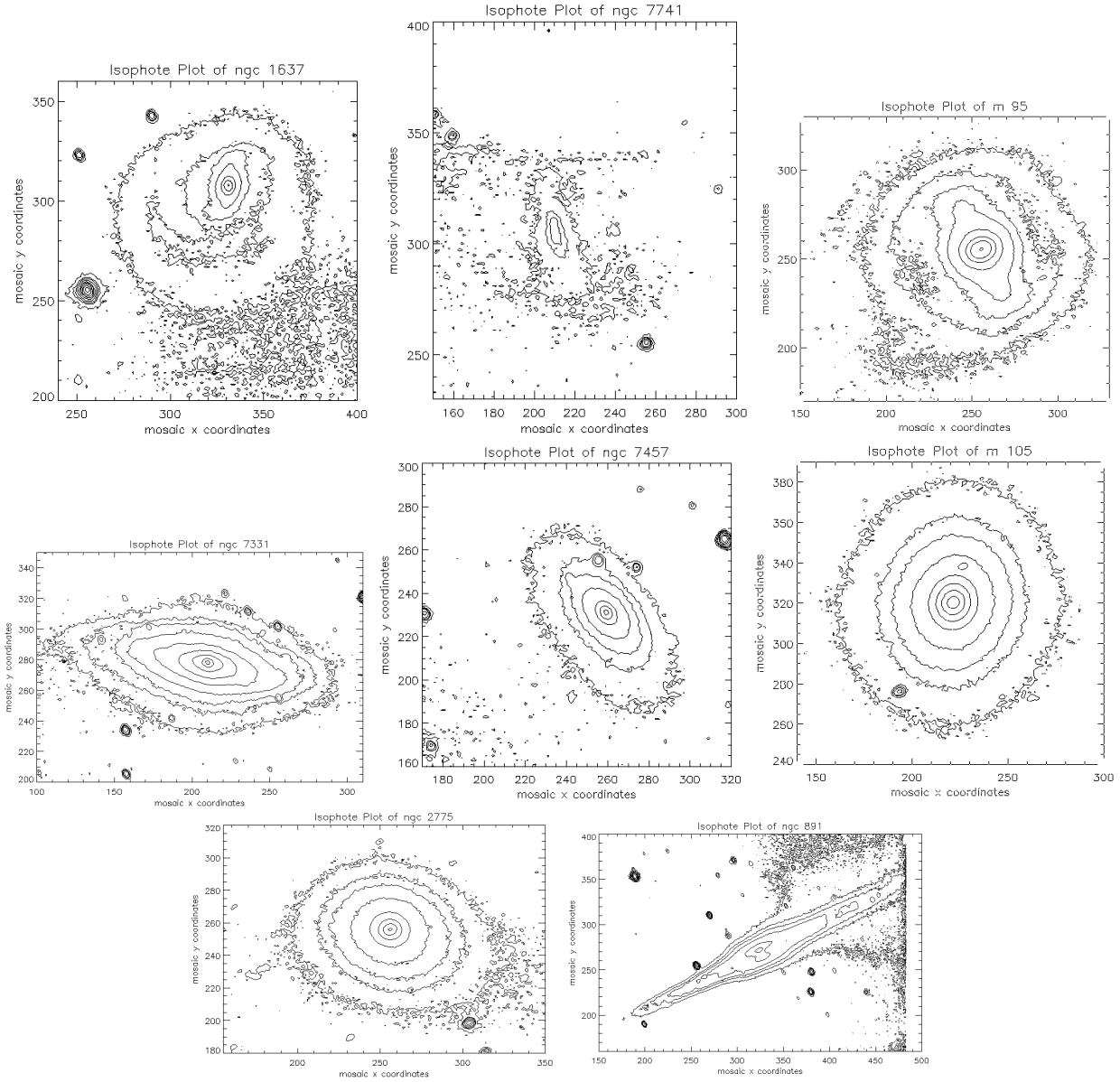

Fig. 5.— From Left to right, top to bottom we have contour plots of scaled according to an integer multiple of rms sky noise counts with outer contour level some minimum integer C times the rms, (C*rms), which marks the approximate edge of the galaxy.:

- (ngc1637: rms = 0.12 C = 2), (ngc7741: rms = 0.13 C = 2), (m95: rms = 0.10 C = 2)
- (ngc7331: rms = 0.12 C = 4), (ngc7457: rms = 0.12 C = 4), (m105: rms = 0.16 C = 2)
- (ngc2775:rms = 0.10 C = 2), and (ngc891: rms = 0.19 C = 3).

Contour Levels scaled according to (C + [0,5,10,20,50,100,200,500,1000])*rms in IDL code notation.

7. Galactic Intensity Profiles

Another useful way to characterize the light from a galaxy is to find its intensity profile. Usually, we assume azimuthal symmetry and plot intensity as a function of radius in (kpc) or (arcmin), which we do here. We could also conceivably plot a histogram of the intensity values for all pixels, which we did not do here.[5] Given a mosaic image, we can find the galactic center and find the average pixel value in $(counts/s)$ in concentric rings about the galactic center. We can then convert this number to magnitudes via our standard star, and further convert it to $mag/\Box''$ to make the galactic astronomers happy. We can then characterize the galaxy's intensity profile in terms of its peak central intensity, and possibly fit the curve to a model. But before we can do this properly, we have to figure out how to determine the physical size of the galaxy so we can plot radius in kpc. We also have to account for the fact that the galaxy may not be face on, but may be inclined along our line of sight. This involves assuming the galaxy to be intrinsically circular and "De-Projecting" it to simulate what we would observe if it was actually face on. We will discuss all these steps and then display and explain the intensity vs. radius plots for all 8 galaxies.

7.1. Physical Sizes of Galaxies

To convert to a physical distance scale for our galaxy we need to know the distance to the galaxy and the angle it subtends on the sky. Given a galactic radius in pixels R_{gal} from our properly tv scaled mosaic image (or our contour plot), we can use the Leuschner plate scale of $(1.82\,''/pixel)$ to convert to the angle θ_{gal} subtended by the galaxy in radians.

$$\theta_{gal}\ (rad) = R_{gal}\ (pixels) \times \left(\frac{1.82\,''}{pixel}\right) \times \left(\frac{1'}{60''}\right) \times \left(\frac{1^o}{60'}\right) \times \left(\frac{\pi\ rad}{180^o}\right) \tag{12}$$

We can estimate the distance to the galaxy using Hubble's law, which for low redshift ($z < 1$) galaxies tells us that a galaxy's velocity is proportional to its distance by the Hubble constant H_o.

$$v = H_o d \quad \Rightarrow \quad d = \frac{v}{H_o} \tag{13}$$

We then look up measured radial velocity values v on SIMBAD, and assume a value for Hubble's constant from (Filippenko, Riess 2000) of $H_o = 65 km/sMpc$. We estimate the error using error propagation and the fact that current published values range from $50 - 80 km/sMpc$, to give a best estimate plus error of $H_o = 65 \pm 15 km/sMpc$. We assume that the error in radial velocity measurement is thus small compared to the error in H_o where the fractional error $\delta H_o/H_o \approx 25\%$. Now that we know the distance to the galaxy d, we can now use the small angle approximation to convert to the physical size of the galaxy, in say kpc.

$$s = d\ \theta_{gal} \tag{14}$$

[5] See Amy Jordan's Lab5 report for Intensity vs. Radius plots for all pixels.

Distances with statistical errors are quoted in a future table for all the galaxies we observed. Regarding systematic errors, presumably, we would measure a galaxy diameter in pixels as larger the more effective exposure time we have in our mosaic, as this would increase the number of stars we can detect at the galactic edge, making the galaxy look fatter in the image. Furthermore, more stars might appear in images taken at other wavelengths, such as the optical, for example. In this sense, when we estimate the physical size of the galaxy from our contour plot or by tv scaling the image and clicking on pixels on opposite ends of the disk, we may be underestimating the true physical size of the galaxy due to the ring of outer stars that are too faint to see in the H band.

7.2. Deprojection

When we look at most galaxies, we see an elliptical shape in the sky. The problem is that the dynamics of stable orbits predict that most stars in the disk of a spiral galaxy, for example, will have circular orbits about the galactic center, leading to a generally circular shape for the disk. If the spiral galaxy is completely face on, we see the galaxy as a circle with inclination angle 0. If the galaxy is inclined at an angle i between our line of sight and the normal to the surface of the galactic disk, we will see it as an ellipse. Thus in order to plot a meaningful intensity profile vs. true galactic radius, we need to simulate the rotation of the galaxy back to a face on position. This is known as "deprojection", and it relies on the assumption that the galaxy disk is intrinsically circular. If we do not deproject, we will underestimate the physical distance for points in the galaxy off the major axis of the ellipse. Points that happen to fall on the major axis are unaffected by the rotation if the major axis is the axis of rotation, as it should be in this case.

The mathematics of deprojection is best illustrated with diagrams, but words and equations will have to suffice here. For an apparent ellipse shaped galaxy with observed major axis a and minor axis b, if we rotate about the major axis, the length of the major axis will remain invariant under that rotation, while the length of the minor axis will appear to shrink. Now the assumption of circularity is equivalent to the claim that the true major and minor axes of the ellipse should be equal. So if the true minor axis of the galaxy is equal to a, but we observe the minor axis to be of length b because the galaxy is inclined at an angle i, simple trigonometry shows us that:

$$cos(i) = \left(\frac{b}{a}\right) \tag{15}$$

Similarly, if we pick an arbitrary point defined with respect to the galactic center that lies at a distance R'_a along the major axis and R'_b along the minor axis, from the Pythagorean theorem, the observed distance from that point to the galactic center R' will be given by:

$$R' = \sqrt{{R'_a}^2 + {R'_b}^2} \tag{16}$$

Now to find the true radial distance R, we need to deproject. Similar trigonometry tells us that $R'_b = R_b\ cos(i)$, and certainly, $R'_a = R_a$, since points along the major axis are unaffected by the rotation. Thus the Pythagorean theorem once again shows us that the true distance R is given by

$$R = \sqrt{{R_a}^2 + {R_b}^2} = \sqrt{{R'_a}^2 + \left(\frac{R'_b}{cos(i)}\right)^2} = \sqrt{{R'_a}^2 + {R'_b}^2 \left(\frac{a}{b}\right)^2} \tag{17}$$

Thus for an arbitrary point on the galaxy, we can measure R'_a, R'_b, a, and b, and determine the true distance R to the galactic center.

The effect of deprojection on our intensity vs. radius plots is this. Without deprojecting, we find the average intensity values in concentric circular rings about the galactic center, which is a reasonable thing to do only if the galaxy is face on (and thus circular) on or inclined by only a small amount. When we deproject, we effectively find our average intensity values in concentric elliptical rings which correspond to the tilted version of the circle we would see if the galaxy were face on. But one must consider the fact that for small inclination angles, the effect of deprojection on your intensity vs. radius plot will be minimal, since for small angles i, $cos(i) = (b/a) \sim 1$, which reduces R to equation 16. However, for inclination angles larger than about 30^o, deprojection becomes quite necessary, as your intensity vs. radius plot would become unphysical if you did not deproject.

It should be noted that the assumption of circularity will introduce a systematic error if the galaxy in question is not intrinsically circular, as is the case for irregular galaxies, lenticular galaxies, and for most ellipticals, which are ellipsoidal in shape. Only for spiral galaxies that have not undergone galactic collisions or large gravitational interactions with neighboring galaxies is the assumption of circularity inherently reasonable. Nevertheless, it will always represent a good first approximation towards deprojecting a galaxy rotated alone our line of sight.

7.3. Bulge and Disk Components

Intensity vs. radius profiles for elliptical and spiral galaxies are empirically observed to fit a few relatively simple curves. For elliptical galaxies, which are essentially ellipsoidal in shape, the observed intensity profile is found to be fit well by a deVaucoleur's law of the form

$$I(R) = I_e \; e^{-7.67[(R/R_e)^{1/4} - 1]} \tag{18}$$

where R_e is a fiducial radius (a free fitting parameter in your model) and $I_e = I(R_e)$.

On the other hand, we have spiral galaxies, which show considerably more structure than ellipticals. The spirals consist of an ellipsoidal bulge component in the center of the galaxy along with a disk containing spiral arms. The bulge of the spiral actually behaves like a "mini-elliptical", in the sense that its intensity profile can be fit well by a deVaucoleur's law. The disk component, on the other hand, is fit better to an exponential given by

$$I_{disk}(R) = I(0) \; e^{-R/h_R} \tag{19}$$

where h_R is the scale length (the distance at which your central intensity value is reduced by a factor of e). So if we want to estimate the total intensity profile of a spiral galaxy, we simply add the bulge and the disk components.

$$I_{spiral}(R) = I_{bulge}(R) + I_{disk}(R) = I_e \; e^{-7.67[(R/R_e)^{1/4}-1]} + I(0) \; e^{-R/h_R} \tag{20}$$

This is a complex non-linear model with 4 free parameters, and as such, we decided it was too complex to try and fit it to our intensity profiles for this lab, and not useful enough to be worth the effort. One can get a qualitative indication of the bulge-disk transition simply by noting where the Intensity vs. Radius curve changes curvature. Similar to the Komolgorov-Smirnoff test from the previous lab, in asking the question "Does this model fit my data?", qualitative considerations are often more practical, at least as a zeroth order approximation.

However, it should be noted that spiral arms do not show up in this model. In fact, if we subtract the actual data from the model, we are left with residuals that contain the spiral arms. This is to be expected because there was nothing built into the model that would take spiral arms into account. And in fact, if we purposely create a model without spiral arms, when we look at the residuals, we actually allow ourselves to examine the spiral structure in ways we could not have done previously. Fitting our data to a model is something we could have done given more time.

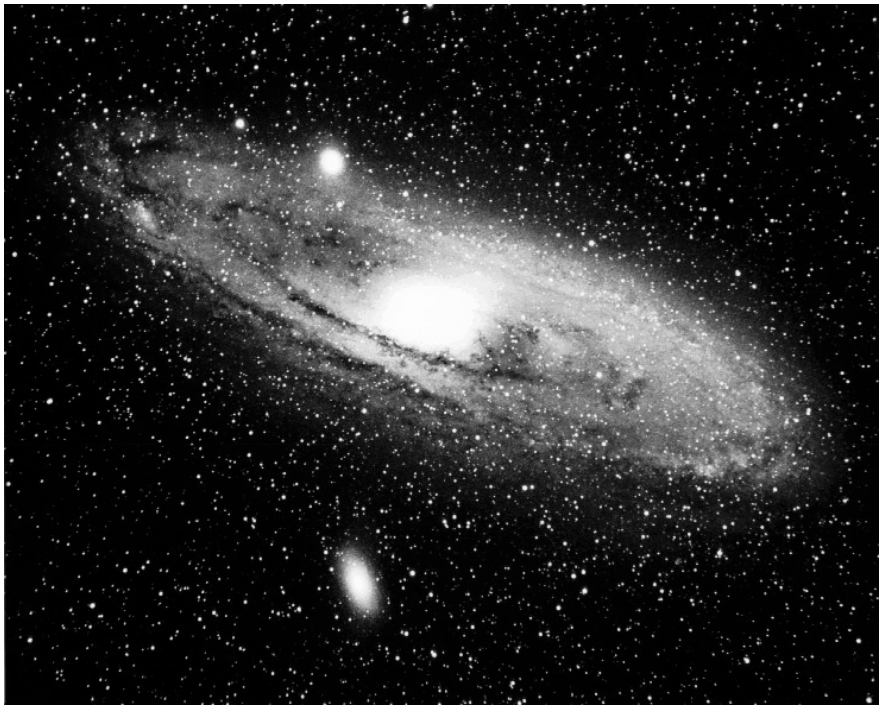

Fig. 6.— Above image of M31, the Andromeda Galaxy, the nearest galaxy to the Milky Way, and possibly the most thoroughly observed an understood spiral galaxy known to astronomers. Notice that due to the inclination angle and close proximity to the galaxy, we can clearly see the bulge, the disk, and the spiral arm components of the galaxy. We can even see dust lanes in the disk as we will see later in the disk of ngc891 for which we create a dust lane extinction map.

7.4. Intensity vs. Radius Plots

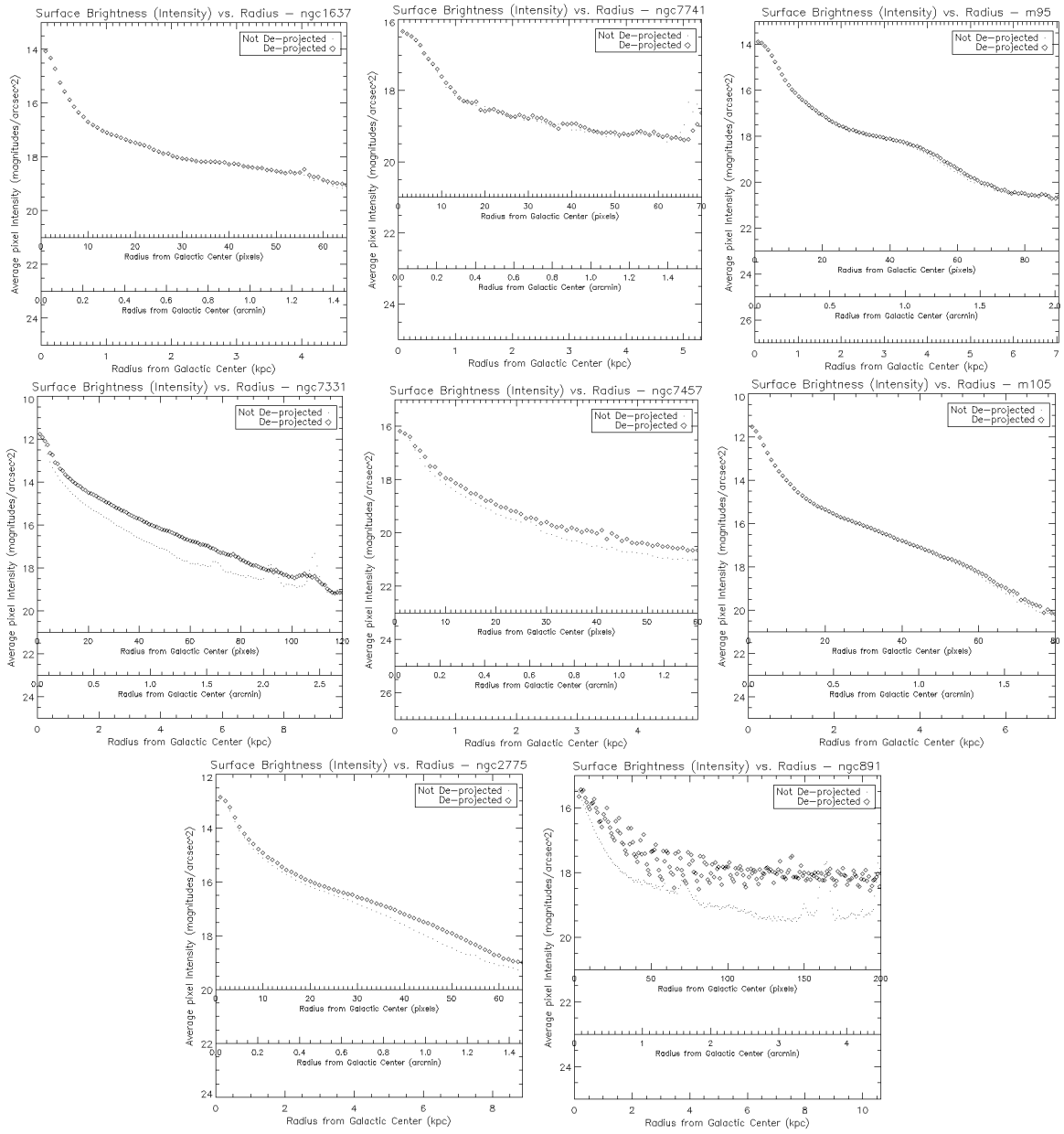

Fig. 7.— From Left to right, top to bottom we have H band Intensity vs. radius plots of:
□ (ngc1637: One Armed Sc Spiral), (ngc7741: Sbc Spiral), (m95: Barred Spiral)
□ (ngc7331: Sb Spiral), (ngc7457: S0 Lenticular), (m105: Elliptical)
□ (ngc2775: S0 Lenticular), and (ngc891:Edge on spiral).
Plots of deprojected intensity for all 8 galaxies in (μ_H) vs. radius in 3 sets of units of (pixels), (arcmin), and (kpc). The ngc891 edge-on plot is noisy as its radial information has been lost.

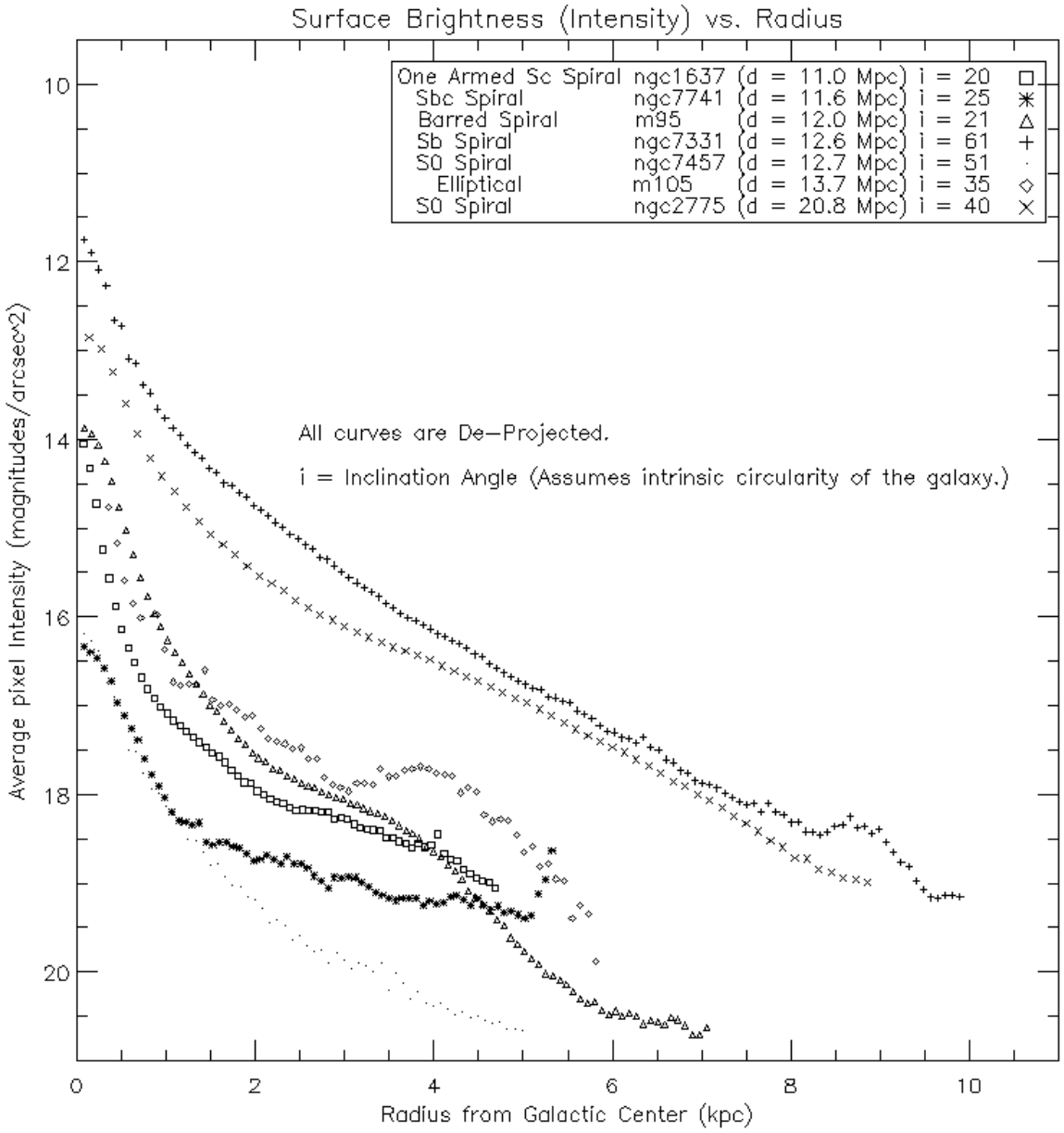

Fig. 8.— Combined Intensity (μ_H) vs radius (kpc) plots for all galaxies except for ngc891. All plots have been deprojected, assuming intrinsic circularity of the galaxy. The physical distance scale of the galaxy is an intrinsic property of the galaxy that can be compared amongst galaxies. Thus we only plot the radius axis in (kpc) since the number of pixels or arcmin subtended by the galaxy is dependent on its distance. Notice also where the bulge and the disk boundary occurs as the curves begin to change slope between roughly 1 and 2.5 kpc. These could in principle be fit with a deVaucoleur's law and an exponential decline. The curve for the elliptical galaxy m105 is suspect. A better m105 plot was shown previously, while this flawed one was not removed from the combined plot. And indeed, as expected, we were able to detect galaxy features as faint as ~ 20 $mag/\Box''$

7.4.1. Summary of Intensity Plot Information

Galaxy Name	Morphology	Distance (Mpc)	Inclination (degrees)	$I_H(0)$ (μ_H)
ngc891	Edge on spiral	8.1 ± 1.9	90 ± 7	—
ngc1637	One Armed Sc Spiral	11.0 ± 2.5	20 ± 3	14.0 ± 0.5
ngc7741	Sbc Spiral	11.6 ± 2.7	25 ± 3	16.3 ± 0.6
m95	Barred Spiral	12.0 ± 2.8	21 ± 3	13.9 ± 0.5
ngc7331	Sb Spiral	12.6 ± 2.9	61 ± 5	11.7 ± 0.4
ngc7457	S0 Lenticular	12.7 ± 2.9	51 ± 5	16.2 ± 0.6
m105	Elliptical	13.7 ± 3.2	35 ± 4	14.0 ± 0.5
ngc2775	S0 Lenticular	20.8 ± 4.8	40 ± 4	12.8 ± 0.4

Table 3: *Galaxy names, morphologies, distances, measured inclination angles, and observed peak intensities toward the galactic center of our observed galaxies, listed in order of increasing distance. Distances found using Hubble's law* $d = \frac{v}{H_o}$, *taking radial velocity values from SIMBAD, and assuming a Hubble constant of* $H_o = 65\frac{km}{sMpc}$. *Distance errors derived using error propagation assuming negligible radial velocity error and an error range for* H_o *of* $\pm 15\frac{km}{sMpc}$. *Inclination angles found assuming the galaxy is intrinsically circular. Inclination errors are statistical random errors involved in measuring the major and minor axes of the apparent galactic ellipse, and do not include systematic error due to the circularity assumption. Intensity errors from error propagation* $\approx$ *3%.*

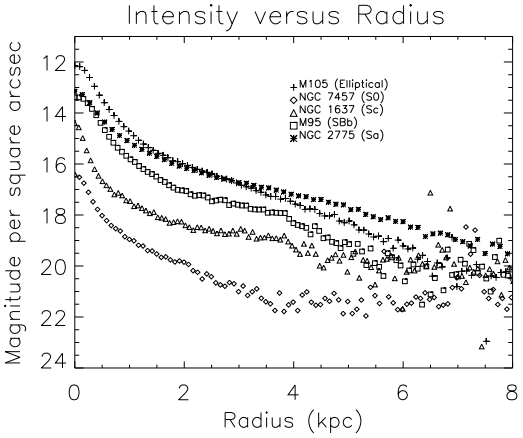

Fig. 9.— For comparison, here are 5 non-deprojected curves of the same galaxies produced by Amy Jordan from the same data. As expected, when we compare plots, the differences only show up in the curves with large inclination angles. The comparison is also useful because it is unclear whether it is valid to deproject the S0 Lenticular galaxies, which may not be intrinsically spherical. Amy did not, but I did and measured high inclination angle of $\sim$ 40 - 50 ^{o}, which may not be physical.

I discerned no obvious correlation between galaxy type, distance to the galaxy, inclination angle, and peak H band intensity. This leads to the conclusion that the intrinsic properties of the galaxies vary enough between galaxies to account for the range of intensity profiles. However inclination will certainly effect the off peak intensity values as a mostly edge-on galaxy will have higher intensities than that same galaxy closer to face on, because our line of sight passes through more stars when the galaxy is edge on. And since the intensity is distance independent, the variation in peak intensity must thus arise from some combination of the measured inclination angle and the intrinsic properties if the galaxy, such as the star density.

7.5. Freeman's Law

Freeman's law is the empirical observation that when one extrapolates the linear portion of the disk component intensity profile of spiral galaxies back to the galactic center, it consistently intersects at a value in the B band of $I_B(0) \approx 21.7\mu_B$. Since we imaged our galaxies in the H band, we must determine what the analogue of Freeman's law should be in the H band. In other words, given $I_B(0) \approx 21.7\mu_B$, we must find $I_H(0)$. We begin with the observed property that galaxies have colors very close to those of K(III) Giant stars. This occurs because even though K(III) giants do not make up the largest number of stars in a galaxy (M.S. stars do), because of their large brightness, they contribute the most to the galaxiy's total luminosity, dominating the galaxy colors. Thus it is a reasonable assumption to use K(III) giant colors to estimate galaxy colors, and a practical one as well since we can use that information to go from B band to H band magnitudes and then convert to $magnitudes/\Box''$. The optical and infrared colors of a representative set of 2 spectral K(III) giant stars is listed in the table below.

Spectral. Type	$U-B$	$B-V$	$V-K$	$J-H$	$H-K$
K3	1.39	1.27	3.0	0.68	0.14
K5	1.81	1.5	3.6	0.79	0.17

Table 4: *The optical UBV and Infrared KHJ colors of some representative K(III) giant star spectral classes (K3 and K5), which we assume to be the colors of our galaxy. Compare this to the lab report which quotes approximate infrared colors of $J-H \approx 0.8$ and $H-K \approx 0.2$. This is closest to the K5 giant, so we will use these specific values in our calculations. (These are de-reddended colors.)*

Thus to go from B to H, we note that $I_B(0) \approx 21.7\mu_B \Rightarrow\ B = m_B = \mu_B + 0.65 = 21.7 + 0.65 \approx 22.35$. Then we use the colors of a K5 giant to find

$$H = B + (H-K) - (V-K) - (B-V) = \ 22.35 + 0.17 - 3.6 - 1.5 \approx 17.42 \qquad (21)$$

This corresponds to an $I_H(0) \approx 17.42 - 0.65 \approx 16.77\mu_H$ and a Freeman's Law in the H-Band of

$$I_H(0) \approx 16.8\ \mu_H \qquad (22)$$

So when we extrapolate the disk component of the spirals we observed back to the galactic center, what sort of peak intensities do we see?

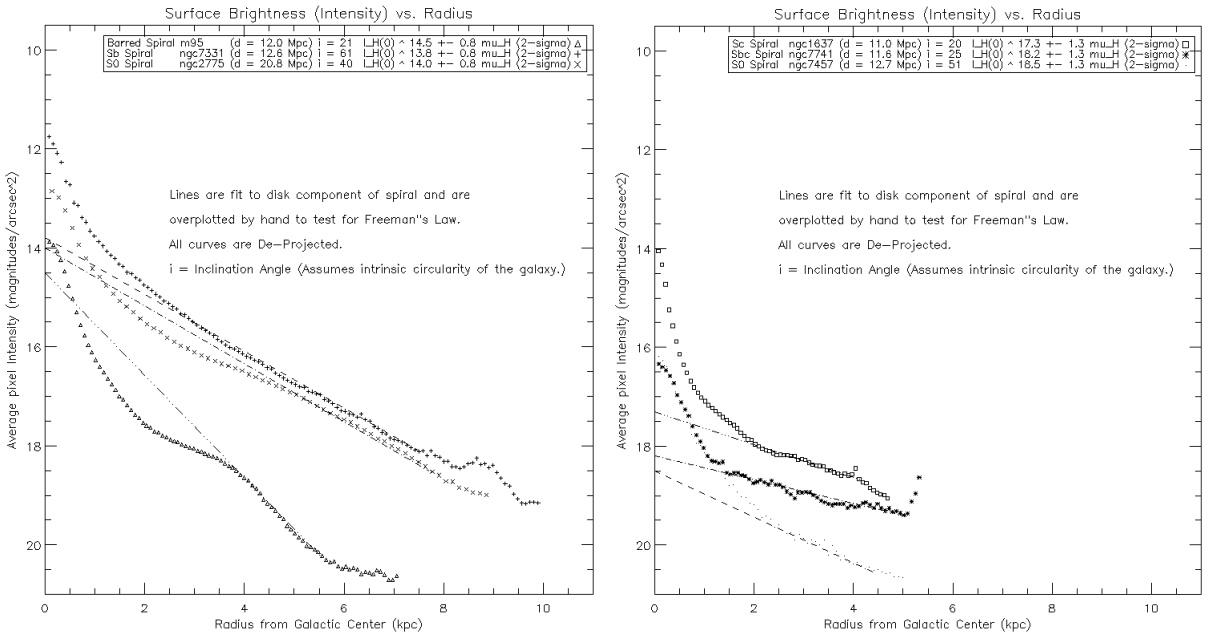

Fig. 10.— Reproducing the intensity vs. radius plots from the previous section here, we find that empirically, the spirals can be broken up into two groups of 3. Each group has a set of disk components that extrapolate back roughly to the same intensity for each grou, the first group with $I_H(0) \sim 18\mu_H$ and the second with $I_H(0) \sim 14\mu_H$. The span of magnitudes is so large here that one can not conclusively say whether Freeman's law holds in the H band. It predicts $I_H(0) \approx 16.8\ \mu_H$, and indeed, the mean of all the intercepts is roughly 16 μ_H. The problem here is that the combined errors in these intercepts from photometry, deprojecting, and most significantly, extrapolating the disk curve to the Intensity axis by hand, are likely to be on the order of $\pm$ 2 - 3 mags.

8. Extinction Map for NGC 891

We imaged the edge on galaxy ngc891 in all 3 bands because it shows a significant dust lane. In order to create an extinction map (or color-color diagram) of the dust lane, we needed to perform galaxy photometry on all 3 bands to generate $J - H$ and $H - K$ colors used to construct the extinction map for ngc891. Using the assumption that the galaxy has the colors of a K(III) giant star $J - H \approx 0.8$ and $H - K \approx 0.2$, we can get a sense of the locus of points that are unreddened by sampling pixels from the bulge. If we then sample pixels embedded within the dust lanes, we can extrapolate back to the locus of unreddened points and use the distance of the line along the reddening vector to estimate the average magnitude of visual extinction A_V intrinsic to the galaxy.

It should be noted that we construct $J - H$ and $H - K$ colors differentially by subtracting mosaics pixel by pixel in the relevant bands. This makes our measurements sensitive to dust within the galaxy but not to intergalactic dust along the line of sight between us and the galaxy. So when we estimate A_V, we are estimating extinction by dust that is intrinsic to the galaxy. To do so, since we do not really have a clear locus of K giant stars as we had for the M.S. locus in lab4, we must estimate the position of the locus in the color-color diagram by other methods. Since we know the reddening vector, we can sample an unreddened distribution of stars from the bulge, and a reddened group from the dust lane, find the centers of each distribution, and fit a least squares line to them with the slope of the reddening vector. Thus the length of the best fit line segment along the reddening vector between the reddened and unreddened locus will give you the average visual extinction in the dust lane. For further details on color-color diagrams, I refer to my Lab4.

For the actual color-color extinction map and a more detailed explanation, I refer to Lee Huss' lab report. In the end, we arrive at an $A_V \approx 7 \pm 1\ mags$.

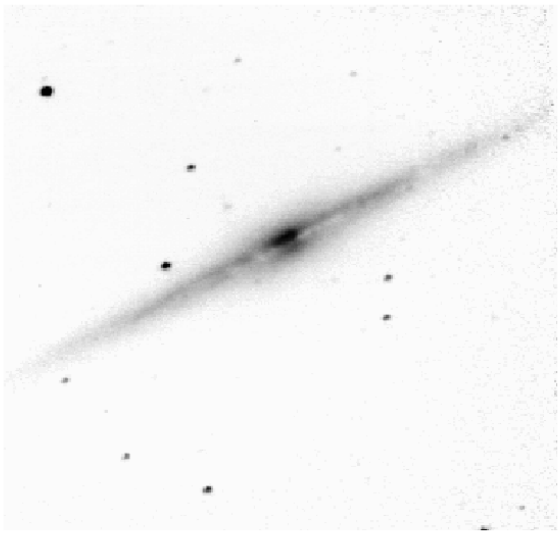

Fig. 11.— Tri-color image of ngc891 reproduced here in grey scale. Notice again the dust lane along the galaxy edge. That's where the action is.

9. Conclusion

Well despite the acid rain, nuclear fallout, and the 5 Tyrannasaurus chasing me at 37 $\frac{miles}{hour}$, I survived. We all did. And I actually will miss it. But at the same time, I'll be glad to stay away from these all nighters, which have already reduced my brain cells down to primordial soup levels. But seriously, great lab Nate. There was a tremendous amount of good stuff packed int here. Extragalactic astronomy is cool and was the natural evolutionary step beyong what we've learned thus far.

In retrospect, this was not a course as much as a way of life, a state of being. And believe it or not, I'm actually interested in doing this astronomy stuff with the rest of my life. Although as a theorist, its a safe bet that I'll get more sleep dammit! And I need that, believe me. But I can never forget the amazing connection between observation and theory. I will be a better theorist for it if I continually look back on the Astro Lab experience and remember. Leuschner will live once again, and 13 ± 5 new kids will be introduced to the joys and sorrow of their new favorite wavelength.

ACKNOWLEDGMENTS

Everybody worked with everybody on this lab, as expected. My lab group size was of the order 10. So I should thank a few people.

See the websites of Amy and Shane for tricolor images of ngc891. I didn't have time to put one up. I focused on deprojection, contour plots, and the generation of the intensity profiles.
Thanks to Lauren and John for helping me create the first mosaics and modify the mosaic software to be able to throw out terrible images.
Thanks to Amy for working with me on generating the intensity vs. radius plots, and Lee for laying the groundwork for the contour plots.
Thanks to Jimbo and John for stellar observationalism, as usual.
Thanks to Lindsey for her conversion of intensity to cgs units.
Thanks to Shane and Eric for working on finding the intensity of the sky, and for letting me quote their values.
Thanks to Lee for generating a rigorous Color-color plot of ngc891 and letting me gaffle the results as well.
Thanks to Nate for writing a kickass lab report, helping out more than his share, and even helping us take data.
Thanks to James for running an amazing course. There's nothing else like it. Even if we go into day trading, we'll still be thinking in idl. Astronomy will never leave us.

Thanks to the galaxies for being there. I'm out.

REFERENCES

1. Lab5 reports of Lee, Amy, Shane, Eric, Lindsey, Jim, and John.

2. *"Allen's Astrophysical Quantities."* Ed. Arthur N. Cox. Pg. 152, Spring 2000 Edition.

3. Carroll Bradley W. and Ostlie, Dale A. *"An Introduction to Modern Astrophysics"*, Addison Wesley, 1996, appendix A15

4. Filippenko A.V., Riess A.G. *"Evidence From Type Ia Supernova for an Accelerating Universe."*, Second Tropical Workshop on Particle Physics and Cosmology: Neutrino and Flavor Physics, ed. J. F. Nieves (New York: American Instit. of Phys.) Aug 2000

5. Graham, James, *"An Infrared Camera for Leuschner Observatory and the Berkeley Undergraduate Astronomy Lab"*, Publications of the Astronomical Society of the Pacific, 113:607-621, 2001 May

6. Graham, James R., *ERRORS & STATISTICS: Ay 122 Lab Notes*, 2001

7. McCrady, Nate., *Lab 5 Handout*, 2001

8. Phillips, A.C. *"The Physics of Stars"* 2nd. ed. John Wiley & Sons, New York, 1999.

9. Taylor, John R., *An Introduction to Error Analysis.* University Science Books, Sausalito, CA 1997, 2nd ed.

10. Woan, G. *The Cambridge Handbook of Physics Formulas* Cambridge University Press, 2000. pg. 177